Brain Structure and Function (2019) 224:2421–2436
https://doi.org/10.1007/s00429-019-01916-7

ORIGINAL ARTICLE

Early trigeminal ganglion afferents enter the cerebellum before the Purkinje cells are born and target the nuclear transitory zone

Hassan Marzban[1,3] · **Maryam Rahimi-Balaei**[1] · **Richard Hawkes**[2]

Received: 24 May 2018 / Accepted: 25 June 2019 / Published online: 29 June 2019
© Springer-Verlag GmbH Germany, part of Springer Nature 2019

Abstract

In the standard model for the development of climbing and mossy fiber afferent pathways to the cerebellum, the ingrowing axons target the embryonic Purkinje cell somata (around embryonic ages (E13–E16 in mice). In this report, we describe a novel earlier stage in afferent development. Immunostaining for a neurofilament-associated antigen (NAA) reveals the early axon distributions with remarkable clarity. Using a combination of DiI axon tract tracing, analysis of *neurogenin1* null mice, which do not develop trigeminal ganglia, and mouse embryos maintained in vitro, we show that the first axons to innervate the cerebellar primordium as early as E9 arise from the trigeminal ganglion. Therefore, early trigeminal axons are in situ before the Purkinje cells are born. Double immunostaining for NAA and markers of the different domains in the cerebellar primordium reveal that afferents first target the nuclear transitory zone (E9–E10), and only later (E10–E11) are the axons, either collaterals from the trigeminal ganglion or a new afferent source (e.g., vestibular ganglia), seen in the Purkinje cell plate. The finding that the earliest axons to the cerebellum derive from the trigeminal ganglion and enter the cerebellar primordium before the Purkinje cells are born, where they seem to target the cerebellar nuclei, reveals a novel stage in the development of the cerebellar afferents.

Keywords Cerebellum · Trigeminal ganglion · Vestibular ganglion · Afferent · Purkinje cell · Cerebellar nuclei

Introduction

The cerebellum has a remarkable afferent topography by which prenatal ingrowing afferents—both climbing and mossy fibers—precisely target a reproducible array of > 100 Purkinje cell (PC) clusters, each comprising a few thousand PCs. Subsequently, these clusters disperse to form the stereotyped adult array of several hundred PC stripes and the afferents remain aligned accordingly (Apps and Hawkes 2009; Leto et al. 2016). This is an extreme example of a general problem in brain development—the precise mapping of afferents onto specific target populations. In many brain regions mapping involves two major steps: a coarse-grained target recognition process based on chemoaffinity and often led by pioneering axons, followed by an activity-dependent, competitive refinement (e.g., cortex: Riccomagno and Kolodkin 2015). In the cerebellum, only the first of these plays a major role: afferent pruning seems unimportant and substantial target field refinement does not appear to take place (e.g., Crepel 1982). Indeed, the broad afferent topography is already in situ at birth (e.g., Reeber et al. 2012;

Electronic supplementary material The online version of this article (https://doi.org/10.1007/s00429-019-01916-7) contains supplementary material, which is available to authorized users.

✉ Hassan Marzban
Hassan.marzban@umanitoba.ca

[1] Department of Human Anatomy and Cell Science, The Children's Hospital Research Institute of Manitoba (CHRIM), Max Rady College of Medicine, Rady Faculty of Health Sciences, University of Manitoba, Winnipeg, MB, Canada

[2] Department of Cell Biology and Anatomy and Hotchkiss Brain Institute, Faculty of Medicine, University of Calgary, Calgary, AB T2N 4N1, Canada

[3] Department of Human Anatomy and Cell Science, Max Rady College of Medicine, Rady Faculty of Health Sciences, University of Manitoba, Rm 129 BMSB, 745 Bannatyne Avenue, Winnipeg, MB R3E 0J9, Canada

Sillitoe 2016). Although extensive pruning certainly occurs in the climbing fiber pathways (e.g., Hashimoto and Kano 2013), this is associated with a transition from multi-innervation to mono-innervation of PCs, not topographical refinement. As a result of this simplification, the development of afferent topography in the cerebellar cortex is a useful model in which to explore the early stages of afferent mapping. The general goal of this study is to identify the earliest afferent projections to the mouse cerebellar primordium and determine which subregion of the primordium they target.

The target of the earliest afferents is the cerebellar primordium. Based on transcription factor expression, four distinct domains can be distinguished: c1–c4 (Chizhikov et al. 2006; Zordan et al. 2008). The c1 domain—also known as the rhombic lip—lies adjacent to the roof plate of rhombomere 1 and is distinguished by the selective expression of atonal transcription factor 1 (Atoh1: Akazawa et al. 1995; Wang and Zoghbi 2001). The c2 domain, also known as the Purkinje cell plate, includes Ptf1a+ and Foxp2+ cells and includes the PCs. The c3 domain—also known as the nuclear transitory zone (NTZ)—lies between c2 and c4 along the entirety of rhombomere 1 except the most rostral end. It contains the glutamatergic CN projection neurons, which selectively express LIM homeobox transcription factor 1 alpha (Lmx1a; Chizhikov et al. 2006) and T box brain gene 1 (Tbr1; Fink et al. 2006). Finally, the c4 domain is located rostrally: it is characterized by LIM homeobox protein (Lhx)1/5 expression (Chizhikov et al. 2006; Zordan et al. 2008), but the fates of c4 cells are unknown.

The conventional view of early cerebellar development is that the first afferent fibers to enter the cerebellar anlage are mossy fibers derived from the vestibular ganglia (Tello 1940). They arrive at around E12 (e.g., in rat, the central processes of the vestibular ganglion neurons are seen at E13 (Morris et al. 1988; Ashwell and Zhang 1992, 1998) and terminate on nascent Purkinje cells in c2. In this report, we provide evidence for a novel earlier stage in afferent development to the cerebellar primordium. We show that axons of the trigeminal ganglion have already entered the cerebellum by E9. This is before the first PCs are born (E10–E13: Miale and Sidman 1961). Rather, they innervate the territory of the CN neurons of c3 (born at E9–E11: Miale and Sidman 1961; Machold and Fishell 2005; Marzban et al. 2014). Only subsequently, at E10/E11, do afferents invade the c2 domain containing the newborn PCs.

Materials and methods

Mice

All animal procedures, in vivo and in vitro, were performed in accordance with institutional regulations and the Guide to the Care and Use of Experimental Animals from the Canadian Council for Animal Care and has been approved by local authorities "the Bannatyne Campus Animal Care Committee" (approved protocol # 15066). In this study, we used embryos from CD1 mice, and neurogenin1 (*Neurog1*) null mutant embryos from timed pregnant mice at E9–E13. Timed pregnant CD1 mice were obtained from Charles River Laboratories (St. Constant, Quebec, Canada), the University of Calgary Animal Resources Centre, and the Central Animal Care Service, University of Manitoba. Animals were kept at room temperature and relative humidity (18–20 °C, 50–60%) on a light and dark cycle (12:12 h) with free access to food and water. The embryo age was determined from the first appearance of a vaginal plug, considered to be E0.5 (all embryo ages in the MS are set to this standard). Mice null for *Neurog1* (Ma et al. 1998) were the generous gift of Dr. Carol Schuurmans (University of Toronto): they were crossed into a CD1 background and compared to normal littermates. Genotyping was performed by polymerase chain reaction as described in Ma et al. (1998).

Antibodies

The following antibodies were used:

- Mouse monoclonal anti-NAA (3A10) recognizes a family of neurofilament-associated antigens (NAA: Bovolenta et al. 1997). We have previously shown anti-NAA immunoreactivity specifically in axons of the cerebellum, both in the adult and during development (Marzban et al. 2008). Anti-NAA antibody was obtained from the Developmental Studies Hybridoma Bank developed under the auspices of the NICHD and maintained by The University of Iowa, Department of Biological Sciences, Iowa City. It was used diluted 1:1000.
- Rabbit polyclonal anti-β-tubulin III antibody recognizes neuron-specific class III β tubulin (Tischfield and Engle 2010) (Cell Signaling Technology, Danvers Mass). It was used diluted 1:500.
- Rabbit polyclonal anti-Lmx1a [the gift of M. German, UCSF: used here as a marker of the c3 domain of the cerebellar primordium (Cai et al. 2009). It is first expressed at E8.5 (Failli et al. 2002)]. The antiserum was generated against a hamster GST-Lmx1a fusion protein. It binds mouse Lmx1a without significant cross-reaction with Lmx1b (Cai et al. 2009) and was used diluted 1:1000.
- Rabbit polyclonal anti-Ptf1a is a marker of the c2 domain of the cerebellar primordium first expressed at E8.5 (Li and Edlund 2001; Lugani et al. 2013). It was the gift of H. Edlund (Umeå University, Sweden) and used diluted 1:1000.
- Rabbit polyclonal anti-Forkhead box (Fox)p2 (EMD Millipore, Billarica, MA, USA). Foxp2 is a marker of

PCs in the c2 domain of the cerebellar primordium (Lai et al. 2003), first expressed at E11 (Lai et al. 2003). The antibody was raised against a GST-tagged recombinant protein corresponding to mouse Foxp2 and used diluted at 1:500.

- Chicken polyclonal anti-T-box Brain Protein 1 antibody (anti-Tbr1). Tbr1 is a neuron-specific T-box transcription factor whose expression during early cerebellar development is restricted to the CN projection neurons of the c3 domain of the cerebellar primordium, first expressed at E10.5–E12.5 (Fink et al. 2006). It was raised against a keyhole limpet hemocyanin-conjugated peptide corresponding to mouse Tbr1 (EMD Millipore, Billarica, MA, USA) and used diluted 1:500.

Immunohistochemistry

Pregnant dams were deeply anesthetized with sodium pentobarbital (100 mg/kg, i.p.) and embryos harvested at the stages of interest and fixed by immersion in 4% paraformaldehyde at 4 °C for 48 h. The embryos were then cryoprotected through a series of buffered 10% (2 h), 20% (2 h), and 30% (overnight) sucrose solutions. Serial series of 20 µm thick sagittal or transverse sections were cut through the extent of the cerebellum on a cryostat and collected on slides for immunohistochemistry. Peroxidase immunohistochemistry was carried out as described previously (Kim et al. 2009; Bailey et al. 2014). Briefly, tissue sections were washed thoroughly, blocked with 10% normal goat serum (Jackson Immunoresearch Laboratories, West Grove, PA, USA) and then incubated in 0.1 M PBS buffer containing 0.1% Triton-X and the primary antibody for 16–18 h at 4 °C followed by a 2 h incubation in horseradish peroxidase-conjugated goat anti-rabbit, anti-chicken or anti-mouse Ig antibodies diluted 1:200 in PBS (Jackson Immunoresearch Laboratories, West Grove, PA, USA) at room temperature. Diaminobenzidine (DAB, 0.5 mg/ml) was used as the chromogen to reveal antibody binding. Sections were dehydrated through an alcohol series, cleared in xylene and cover slipped with Entellan mounting medium (BDH Chemicals, Toronto, ON, Canada). Embryonic sections for double-label fluorescent immunohistochemistry were processed as described previously (Bailey et al. 2014). Briefly, tissue sections were washed, blocked in PBS containing 10% normal goat serum (Jackson Immunoresearch Laboratories, West Grove, PA, USA) and incubated in both primary antibodies overnight at room temperature, rinsed, and then incubated for 2 h at room temperature in a mixture of Alexa 546-conjugated goat anti-rabbit Ig and Alexa 488-conjugated goat anti-mouse Ig (Molecular Probes Inc., Eugene, OR, USA), both diluted 1:2000. After several rinses in 0.1 M PBS, sections were cover slipped in non-fluorescing mounting medium (Fluorsave Reagent, Calbiochem, La Jolla, CA, USA). Whole mount peroxidase immunocytochemistry was performed according to Sillitoe and Hawkes (2002) except that the PBS containing 5% skim milk (Nestlé Foods Inc., North York, ON, Canada) plus 0.1% Triton-X 100 (Sigma, St. Louis, MO, USA) was used as blocking solution. Biotinylated goat anti-rabbit IgG (Jackson Immuno Research Labs Inc., West Grove, PA, USA) was diluted 1:1000 in PBS containing 0.1% Triton-X 100 and incubated with the embryos overnight. Embryos were washed with PBS (3 × 2 h) and subsequently incubated overnight with ABC complex solution prepared according to the manufacturer's instructions (Vectastain, Vector Laboratories Inc., Burlingame, CA, USA). Antibody binding was revealed using DAB as the chromogen.

Embryo cultures

Embryo cultures were prepared from E9 CD1 timed pregnant mice. Each embryo was removed from the amniotic sac and immediately placed in ice-cold Ca^{2+}/Mg^{2+}-free HBSS containing gentamicin (10 µg/ml) and 6 mM glucose. After positioning the embryos on a membrane (Kimtech Science, Roswell, GA, USA), they were placed into 24-well plates in culture medium supplemented with 10% fetal bovine serum at 100% humidity at 37 °C in 5% CO_2 and maintained in vitro for 4 days (DIV).

Axon tracing

To visualize axons extending from the trigeminal ganglion to the cerebellar, primordium dye tracing was carried out according to Ashwell and Zhang (1998). Embryos from timed pregnant dams were immersion fixed in 4% PFA at 4 °C for 2–5 days. One or two crystals of the carbocyanine dye DiI (1,1′-dioctadecyl-3,3,3′,3′-tetramethylindocarbocyanineperchlorate), ~ 150 µm in diameter, were inserted into a trigeminal ganglion of embryos at ages E10 and E11 ($N = 5$ each). The trigeminal ganglion was identified by its gross morphology and location, either side of the rostral rhombencephalon and ventral to the angle of the junction between the rostral and the caudal rhombic lips (see asterisk in Fig. 6b). They were then returned to the fixative and stored in the dark at 37 °C for up to 8 weeks.

Imaging and figure preparation

For bright-field microscopy, images were captured using a Zeiss Axio Imager M2 microscope (Zeiss, Toronto, ON, Canada). For low magnification fluorescence microscopy, a Zeiss Lumar V12 Fluorescence stereomicroscope (Zeiss, Toronto, ON, Canada) equipped with a camera was used. Images were analyzed using Zen software. For high magnification fluorescence microscopy, a Zeiss Z1 and Z2 Imager and a Zeiss LSM 700 confocal microscope (Zeiss, Toronto,

ON, Canada) equipped with camera and Zen software were used to capture and analyze images. Images were cropped, corrected for brightness and contrast, and assembled into montages using Adobe Photoshop CS5 Version 12.

Results

Development of the embryonic cranial nerves

To follow the development of the embryonic cranial nerves and their projections to the cerebellum, sections through the cerebellar primordium were immunostained with an antibody that recognizes neurofilament-associated antigen (NAA). Anti-NAA is an excellent tool to reveal the distribution of many afferents in the cerebellum (e.g., Marzban et al. 2008). Homogenates of the E10, E11, and E12 cerebellum separated by polyacrylamide gel electrophoresis, Western blotted, and probed for NAA immunoreactivity revealed the expected single band of apparent molecular weight ~200 kDa (Fig. 1a; Marzban et al. 2008). High magnification views indicate that NAA immunoreactivity is localized primarily in axons (Fig. 1b) but occasional weakly immunoreactive (NAA+) somata are seen (data not shown). To confirm this localization, cerebellar sections were double immunofluorescence stained for NAA and the neuron-specific marker β-Tubulin III (Moody et al. 1989): the two markers are co-expressed (Fig. 1c–e). The NAA results were also replicated by immunostaining for a second anti-neurofilament antigen (SMI-32; Lin et al. 2004; data not shown).

Most cranial nerves originate from the brain stem and have both sensory and motor components. The sensory components, including the ganglia, are born early in development (~E9) and have a dual origin: the distal portions are placodal derivatives and the proximal parts are of neural crest cell origin (Hamburger 1961; Streit 2004; Schlosser 2006). To reveal the distribution of NAA immunoreactivity in the embryonic brain, timed embryos were immunoperoxidase stained in whole mount. At E10, NAA immunoreactivity characteristic of phosphorylated neurofilaments is strongly present in both the neuronal somata and axons of the cranial and spinal nerves and ganglia (Fig. 2a, b). In the brain stem, neurons of the epibranchial placodes that comprise the distal parts of the facial (VIIth or geniculate), glossopharyngeal (IXth or petrosal) and vagus (Xth or nodose) cranial nerve ganglia are all NAA+ (Fig. 2a, b). NAA immunoreactivity is also strongly expressed in the trigeminal placode, which lies caudal to the mesencephalon and rostral to

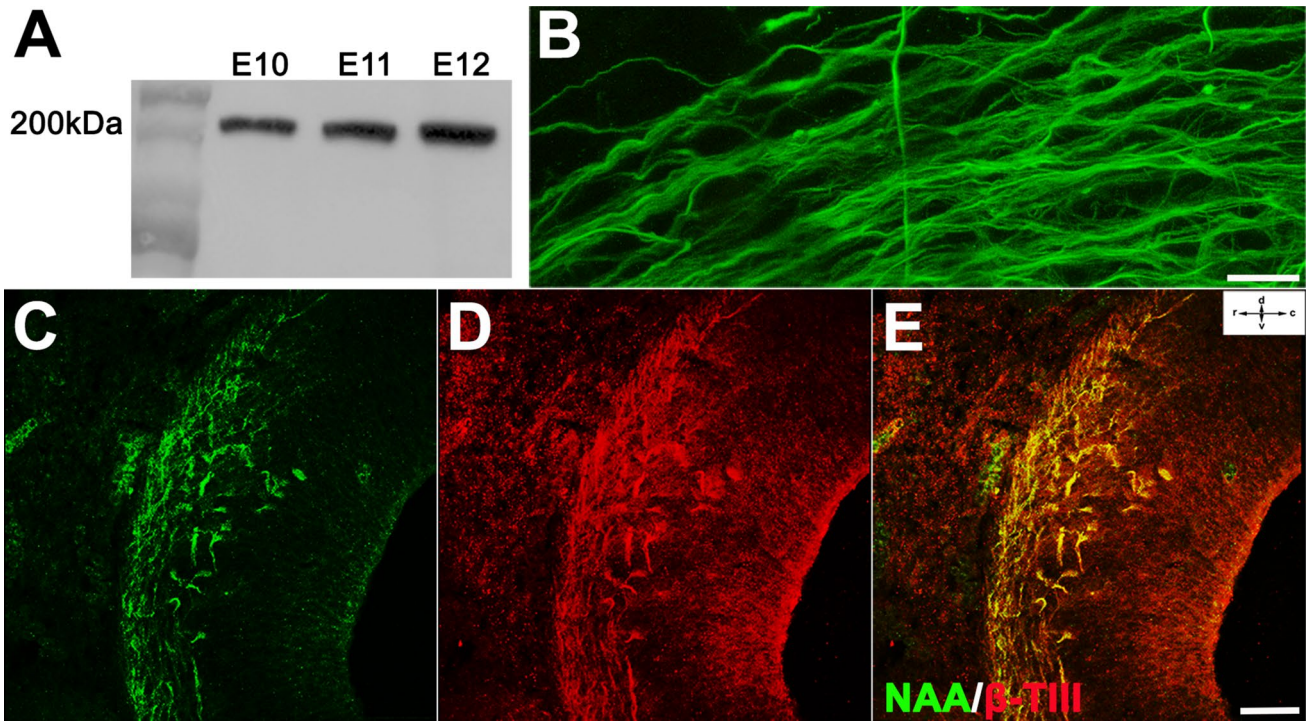

Fig. 1 The expression of neurofilament-associated antigen (NAA) in the embryonic cerebellum. **a** Western blots of cerebellar homogenate from the E10, E11, E12 mouse probed with anti-NAA and compared to molecular weight standards (s). The expected single polypeptide band is revealed, with apparent molecular weight ~200 kDa. **b** High magnification image of sagittal section through the cerebellar primordium at E10. Immunofluorescence staining indicates that the NAA immunoreactivity is associated with axons. **c–e** A 20 µm sagittal section through the E10 lateral cerebellar primordium double immunofluorescence stained for NAA (**e**—green) and β-tubulin III (β-T-III: **f**—red; **g**—merged). NAA is co-expressed with β-tubulin, consistent with an axonal location. Scale bar: 10 µm in **b**; 100 µm in **c–e**

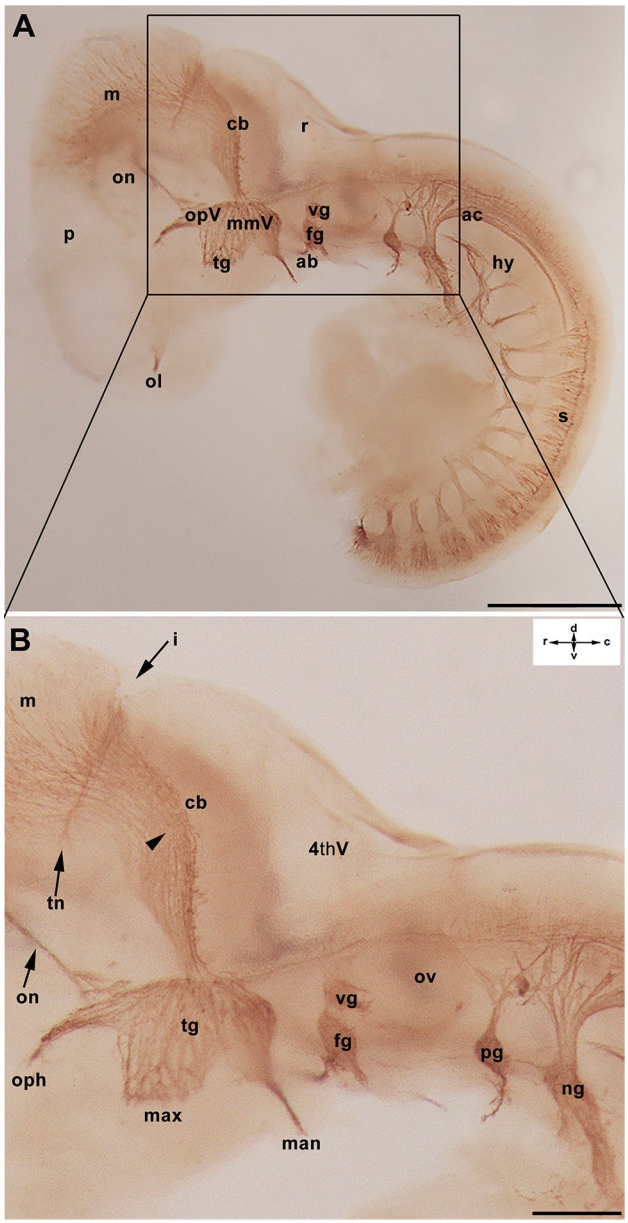

Fig. 2 The cranial nerves in the developing mouse embryo at E10 are revealed by the expression of NAA. **a**, **b** Whole mount anti-NAA immunostaining at E10 from the region outlined in the inset (**a**) shows the developing cranial nerves with a particular focus on relationships between the trigeminal (tg), facial (fg), and vestibular (vg) ganglia and the cerebellar primordium (cb). The central trigeminal ganglion projection to the cerebellar primordium is indicated by the arrowhead. The isthmus (i) and the trochlear nerve (tn) indicate the approximate location of the mesencephalic–metencephalic boundary. Additional abbreviations: *4thV* 4th ventricle, *ab* abducens nerve, *fg* facial ganglion (=geniculate ganglion), *hy* hypoglossal nerve, *man* mandibular nerve, *max* maxillary nerve, *m* mesencephalon, *mmV* maxillomandibular placode, *ng* nodose ganglion (=vagus ganglion), *on* oculomotor nerve, *ol* olfactory nerve, *oph* ophthalmic nerve, *opV* ophthalmic placode, *ov* otic vesicle, *p* prosencephalon, *pg* petrosal ganglion, *r* rhombencephalon, *s* spinal cord. Scale bar: 500 µm in **a** and 200 µm in **b**

the rhombencephalon and forms the large trigeminal ganglia. The trigeminal ganglion arises from two distinct subplacodes, the ophthalmic (opV) and the maxillomandibular (mmV) (Lassiter et al. 2014), which are shown at E10 in Fig. 2b and are clearly distinguishable from E9 (see Fig. 6a, b). The peripheral projections of the trigeminal ganglion—the ophthalmic, maxillary and mandibular nerves—follow distinct routes from the outset. The centrally directed axons appear to extend rostrally to the cerebellar primordium and mesencephalon and caudally to the rest of the rhombencephalon and the upper cervical spinal cord.

Axons from the trigeminal nerve are the first to project to the cerebellum

To identify the earliest cerebellar afferents, whole mount and section immunohistochemistry was performed on mouse embryos at E9, the earliest that the cerebellar primordium can be anatomically identified reliably (Fig. 3; Fig. Suppl. 1) and E11 (Fig. 4). The boundaries of the cerebellar primordium are not well defined anatomically. For present purposes, we follow Altman (Altman and Bayer 1985) and consider the primordium to be located in the dorsorostral face of the 4th ventricle, dorsal to the point of entry of the trigeminal nerve, rostral to the rhombic lip, and caudal to the isthmus (e.g., Fig. Suppl. 2). Medially, the rostral boundary is also indicated by the path of the trochlear nerve (e.g., Figs. 2b, 4a, 7a, c). In more lateral sections, the cerebellar primordium is crescent shaped (see Figs. 1c–e, 4c–f; Fig. Suppl. 2C, D), corresponding to Altman's "lateral cerebellar primordium" (Altman and Bayer 1985). This definition encompasses the locations of the Purkinje cell plate (c2) and the nuclear transitory zone (c3), as identified by Foxp2/Ptf1a and Tbr1/Lmx1a expression, respectively (see Figs. 8, 9, 10; Fig. Suppl. 2 A, B).

At E9, NAA immunohistochemistry shows that the trigeminal ganglion and its central axons to the cerebellar primordium (rhombomere 1) are already present (Fig. 3a, arrow). The peripheral ophthalmic projection and the facial ganglia are also NAA+ by E9 (Fig. 3a, arrowhead), but the vestibular ganglia are not yet seen (Fig. 3c–f: their future location, adjacent to the otic vesicle, is indicated by the arrow in Fig. 3c: they are present by E10—see Fig. 2a, b). The centrally directed axons of the trigeminal ganglion bifurcate upon entry into the brainstem and elongate to form the ascending (arrow) and descending (arrowhead) branches of the trigeminal tract (Fig. 3f) (Erzurumlu and Jhaveri 1992). At this stage, the ascending tract presents as a bundle running rostrally across the dorsomedial surface of the cerebellar primordium. In some cases, two fascicles can be discerned (Fig. 3e, arrow), which may the precursors of the clearly differentiated fascicles seen by E11 (Fig. 4c–f). At high magnification, the ascending

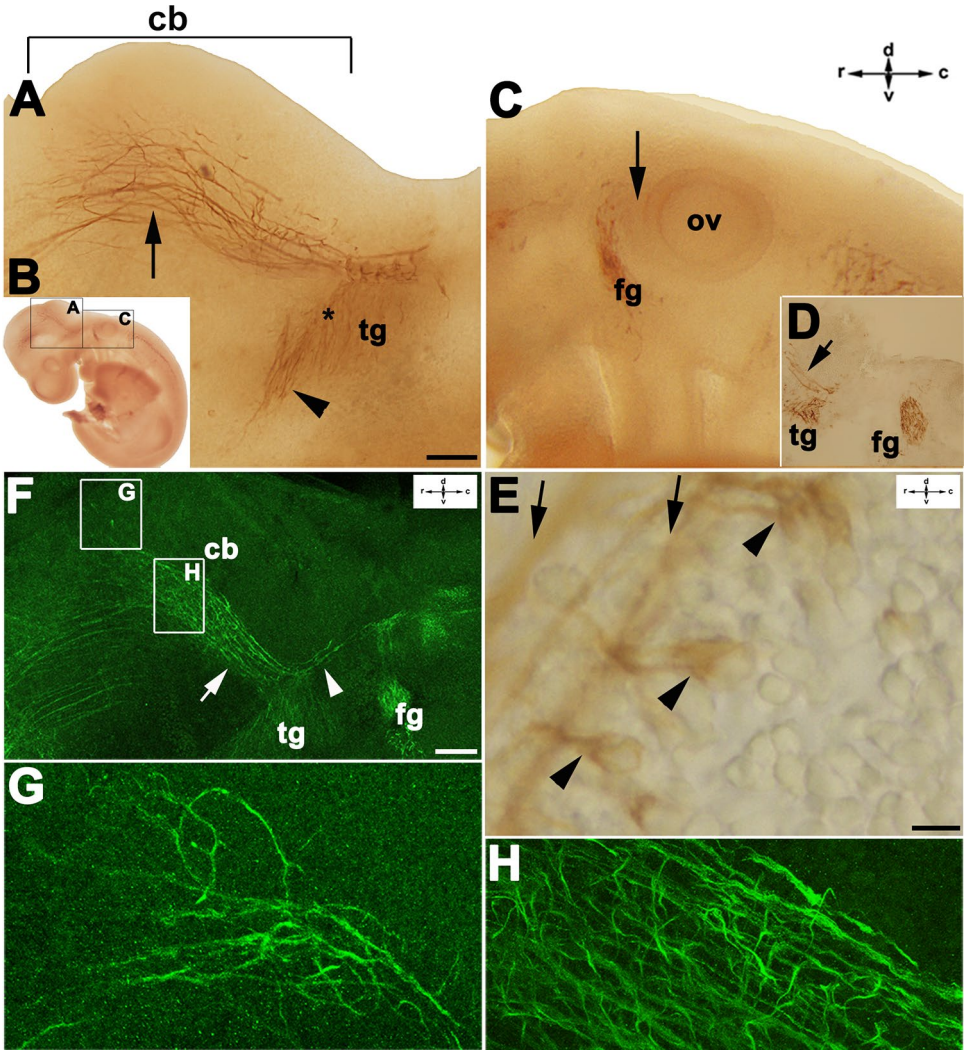

Fig. 3 The cranial nerves in the whole mount mouse embryo at E9 immunostained for NAA. **a** Immunoperoxidase staining of the projection from the trigeminal ganglion (tg) to the cerebellar primordium (cb) at E9, taken from the region indicated in the inset (**b**). The central NAA+ axons extend dorsally to form a bundle (arrow) that continues rostrally to the cerebellar primordium. The ophthalmic peripheral projection from the trigeminal ganglion is indicated by the arrowhead and the ophthalmic placode by an asterisk. **c** Caudal to **a** (the region indicated as **c** in the inset **b**) peroxidase reaction product is deposited in axons of the facial ganglion (fg). The vestibular ganglion has not yet formed. Its future location, between the facial ganglion and the otic vesicle (ov), is indicated by the arrow: see also E10 (Fig. 1) and E11 (Fig. 3). **d** An E9 20 µm sagittal section through the rhombencephalon (region indicated as **c** in **b**) immunoperoxidase stained for NAA to show the facial and trigeminal ganglia and the rostral projection (arrow) towards the cerebellar primordium (cb). **e** High magnification image of a lateral sagittal section through the cerebellar primordium at E9, immunoperoxidase stained for NAA to show the two NAA immunoreactive fascicles (arrows). The arrowheads indicate weakly immunoreactive profiles that are either axon hillocks of the nascent CN neurons or early afferents terminating on CN somata. **f–h** Confocal microscopy images of whole mount E9 mouse embryos at low magnification (**f**) immunofluorescence labeled for NAA to show the ascending (arrow) components of the trigeminal ganglion-derived fibers in the rostromedial (**g**), and caudolateral cerebellar primordium (**h**). The arrowhead indicates the descending trigeminal ganglion-derived fibers towards the spinal cord. Scale bars: 100 µm in **e**; 20 µm in **f–h**

trigeminal axons are seen in the most rostromedial (Fig. 3f, g) and subpial (Fig. 3f, h) regions of the cerebellar primordium: the c1–c4 divisions—see "Introduction"—are not well defined at E9 but likely this represents the nascent c3 (compare to Figs. 8 and 9, in which c3 is well developed). The descending components of the trigeminal fibers are located between the trigeminal ganglion and the facial nerve in the alar plate of r3/4 (Fig. 3f, arrowhead).

By E11, NAA immunoreactivity clearly reveals the trigeminal, facial, and vestibular ganglia caudal to the cerebellar primordium, together with their peripheral and central projections (Fig. 4a–d, f). In particular, the central axons of

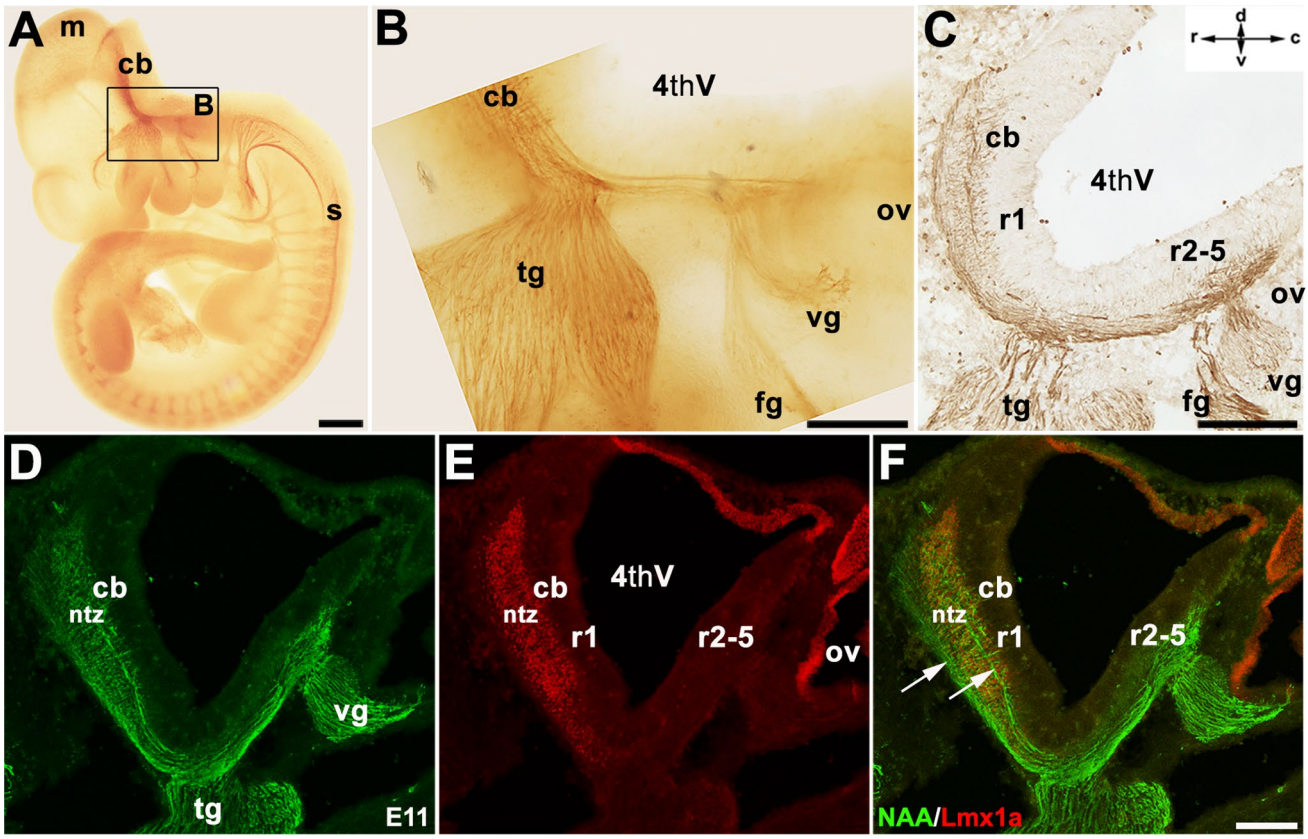

Fig. 4 The cranial nerves in the developing mouse embryo at E11 in whole mount immunoperoxidase stained for NAA. **a** Low magnification view of an NAA immunoperoxidase-stained embryo at E11. **b** Higher magnification view of the region outlined in "**a**" shows the trigeminal (tg), facial (fg) and vestibular (vg) ganglia. The newly formed vestibular ganglion lies between the facial ganglion and the otic vesicle (ov). An NAA+ axon bundle extends from the ganglia towards the neuroepithelium of the 4th ventricle (4thV) and then rostrally to the cerebellar primordium (cb) and caudally towards the spinal cord. The NAA+ axons between the trigeminal and vestibular ganglion comprise the descending axons from the trigeminal ganglion and ascending axons of the vestibular ganglion and spinal cord afferents. **c** A 20 µm lateral sagittal section through the rhombencephalon at E11 immunoperoxidase stained for NAA. Reaction product is deposited in axons of the developing trigeminal, facial and vestibular ganglia and their central outgrowth to the cerebellar primordium (alar plate of rhombomere (r) 1). **d**–**f** Double immunofluorescence staining for NAA (**d**—green) and Lmx1a (**e**—red; **f**—merged) of a lateral sagittal section at E11 showing the trigeminal (tg) and vestibular (vg) ganglia and their central pathway to the cerebellar primordium [alar plate of rhombomere 1 (r1)] and the nuclear transitory zone (ntz). Two distinct NAA+ axon fascicles are seen in the cerebellar primordium, indicated by the arrows in "**f**". Scale bars: 500 µm in **a**; 200 µm in **b**, **c**; 200 µm in **f** applies also to **d**–**f**

the trigeminal ganglion are directed rostrally into the cerebellar primordium (Fig. 4b–d, f) and probably continue on to the mesencephalon (Fig. 4a), and caudally through the caudal rhombencephalon (Fig. 4b–d, f) towards the developing spinal cord. The NAA+ axons appear to comprise two discrete fascicles, the one from the trigeminal ganglion seen superficially, close to the pial surface, from E9 onwards and a second, narrower fascicle, possibly present from E9/10 (e.g., E9—Figs. 3e, 6b; E10—Fig. 9j) and seen clearly by E11 (Fig. 4c, d, f, arrows). The latter runs more deeply and terminates in both c3 and extends collateral branches that innervate c2 (Figs. 3c, f, 9f, i, 10f, g). Whether the deeper nerve fibers also derive from the trigeminal ganglion, perhaps representing the deeper fascicle noted at E9/E10, which has displaced ventrally as the cerebellar primordium reorganizes, is unclear. However, because of the close functional and anatomical relationships between cranial nerves V and VII (Sanders 2010), we cannot exclude facial nerve involvement.

Do the axons of the trigeminal ganglion project directly to the cerebellum in the embryonic mouse?

To test the hypothesis that NAA+ axons in the cerebellar primordium at E9–E11 derive from the trigeminal ganglion, we have pursued three independent strategies—DiI tract tracing, analysis of the *Neurog1*$^{-/-}$ mouse in which the trigeminal ganglion never forms, and whole mount cultures of the developing embryo in vitro in which an alternative potential source of the early cerebellar afferents, the mesencephalic

trigeminal nucleus (MesV) (Billig et al. 1995), does not develop (Marzban, H: unpublished data).

First, DiI crystals were applied to one trigeminal ganglion of paraformaldehyde-fixed embryos at E10 and imaged 4–8 weeks later using confocal microscopy. Care was taken to ensure that diffusing DiI did not impinge upon the nascent vestibular ganglion. Tightly bundled axons were seen pursuing a rostral course across the dorsum of the cerebellar primordium, immediately beneath the pial surface (Fig. 5a–c). This supports the hypothesis that the trigeminal ganglion projects directly to the embryonic cerebellar primordium and that the axons seen in the primordium at E10 include those from the ipsilateral trigeminal ganglion.

Second, we wished to confirm that the axon tract between the trigeminal ganglion and the cerebellar primordium derives from the central ganglion and not, for example, descending axons from MesV. The trigeminal ganglion is the largest of the cranial sensory ganglia. Their neurons are of both placodal and neural crest origin, both of which depend for their development on the proneural transcriptional regulator *Neurog1*, and elimination of *Neurog1* by homologous recombination prevents the development of both trigeminal and vestibular ganglia (Ma et al. 1998; Fode et al. 1998; Ma et al. 1999, 2000; Karpinski et al. 2016). Thus, to confirm that the anti-NAA immunostained axons in the cerebellar primordium at E9 derive from the trigeminal system, we investigated the early cerebellar axons in the *Neurog1* null mouse (Fig. 6). Whole mount NAA immunoperoxidase staining in an E9 control (Fig. 6a, b) and a *Neurog1*$^{-/-}$ littermate (Fig. 6c, d) shows the complete lack of the trigeminal

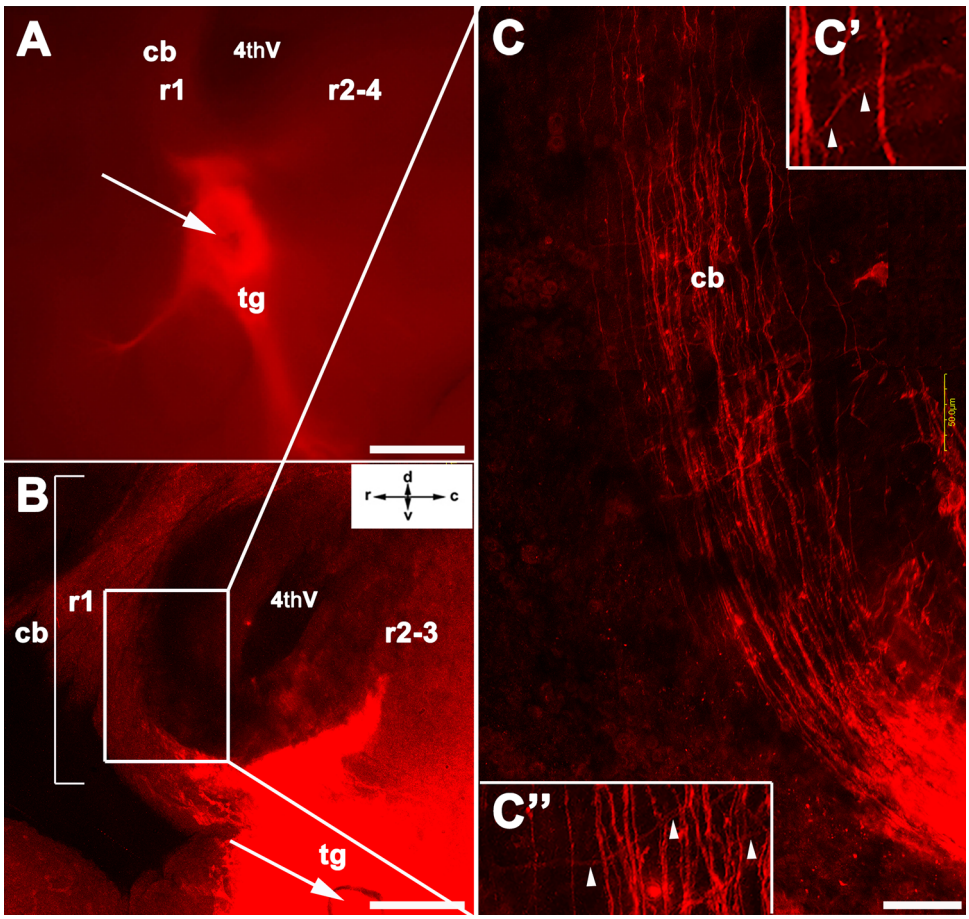

Fig. 5 DiI tracing of the projection from the trigeminal ganglion to the cerebellar primordium at E10. **a** A DiI crystal (arrow) was inserted to the trigeminal ganglion (tg) of a paraformaldehyde-fixed E10 mouse embryo and imaged 3 days later using stereomicroscopy to show the location of the DiI crystal in the trigeminal ganglion. Labeled axons extend rostrally towards the 4th ventricle (4thV) and the cerebellar primordium (cb). **b** One month later, the intact embryo was mounted in glycerin, cover slipped and imaged using confocal microscopy. The arrow shows the location of the DiI crystal in the trigeminal ganglion. The trigeminal ganglion was filled, but the DiI did not diffuse as far as the vestibular or facial ganglia (in the area adjacent to r2–3). A DiI-stained axon projection is seen extending from the trigeminal ganglion around the 4th ventricle (4thV) into the cerebellar primordium (cb). **c**, **c**', **c**" A high magnification view of the DiI labeled axon tract between the trigeminal ganglion and the cerebellar primordium showing individual branching axons running perpendicular to the main axonal projection. **c**', **c**" High magnification views from **c** with putative collateral branches indicated by arrowheads. Scale bars: 500 µm in **a**; 250 µm in **b**; 50 µm in **c**

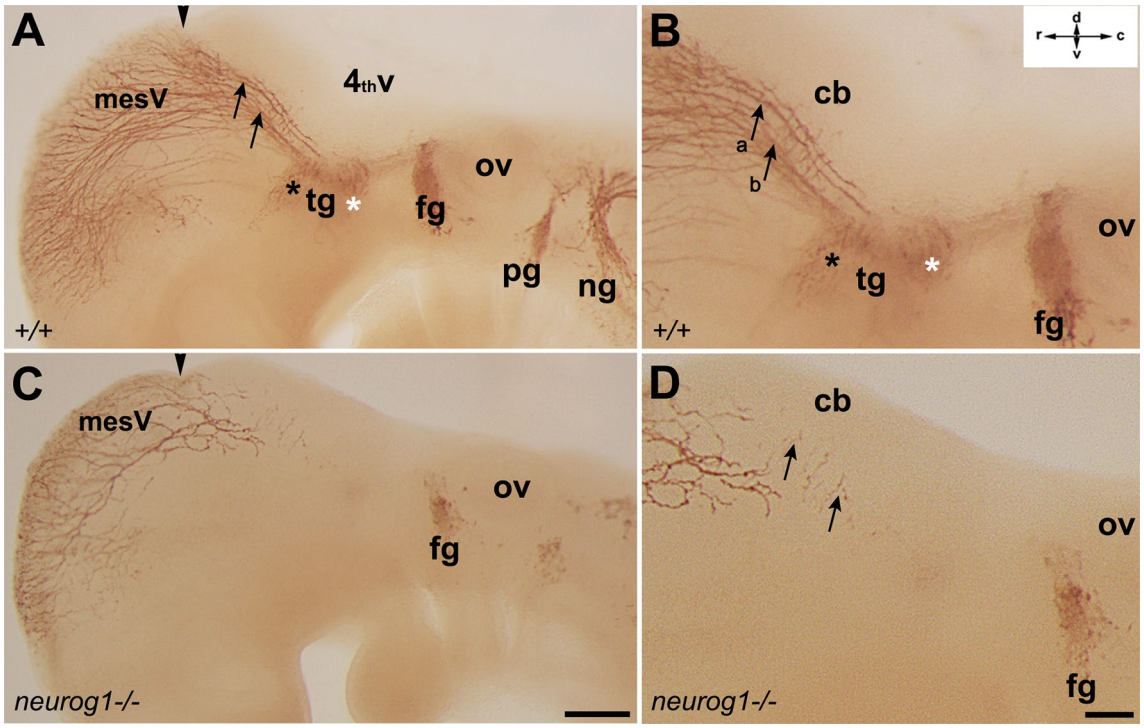

Fig. 6 Whole mount NAA immunoperoxidase staining of *Neurog1*$^{-/-}$ and control (+/+) littermate embryos at E9. **a** In the +/+ embryo in the region of the 4th ventricle (4thV), the trigeminal (tg) and facial (fg) ganglia are strongly immunoreactive and NAA+ axons are seen within the cerebellar primordium (cb: arrow). The subregions of the trigeminal placode, the ophthalmic placode and the maxillomandibular placode, are indicated by black and white asterisks, respectively. The vestibular ganglion has not yet developed between the facial ganglion and the otic vesicle (ov). In addition, numerous NAA+ axons are present in the mesencephalic trigeminal nucleus (MesV) (arrowhead indicates the isthmus). **b** A high magnification view of the embryo in A ("a" and "b" indicate axon fascicles). **c** In the *Neurog1*$^{-/-}$ embryo afferents from MesV are present at the rostral end of the cerebellar primordium. The trigeminal and vestibular ganglia are absent and the cerebellar primordium lacks all ascending afferents (arrowhead indicates the isthmus). **d** A high magnification view of the embryo in **c**. The rostral cerebellar primordium contains a sparse projection from MesV (arrow) but nothing from the caudal cranial ganglia. Scale bars: 200 µm in **a**, **c**; 100 µm in **b**, **d**

ganglion in the *Neurog1*$^{-/-}$ embryo. In the cerebellar primordium, both the superficial and deep NAA+ axon tracts are absent. The vestibular ganglia are also absent, but other cranial ganglia, for example, the facial ganglion—Fig. 6c, d) develop normally: likewise, the extensive axon ramifications of MesV also appear unaffected (compare +/+ in Fig. 6a to *Neurog1*$^{-/-}$ in Fig. 6c). The *Neurog1*$^{-/-}$ cerebellar primordium shows only a few rostral NAA+ axons at E9 (Fig. 6c, d), while in control littermates, the superficial axon tract in the primordium is strongly NAA+ (Fig. 6a, b), consistent with the hypothesis that the axon tract between the trigeminal ganglion and the cerebellar primordium derives from the trigeminal ganglion rather than from MesV. Despite the finding that the prominent NAA+ axon tract between the trigeminal ganglion and the cerebellar primordium derives from the trigeminal ganglia, NAA immunostaining of the *Neurog1*$^{-/-}$ embryo still indicates the presence of sparse, weak NAA+ axons, oriented orthogonal to the surface of the 4th ventricle, in the rostral cerebellar primordium (e.g., Fig. 6d, arrow). These appear to reflect NAA expression by the nascent axons of the CN neurons in c3 (see Figs. 3e, 6d: for NAA+ CN neurons at E12, see Fig. 9g and E10, Fig. 9j, arrow).

Third, to test the hypothesis that the earliest cerebellar afferents derive not from the trigeminal ganglion but rather are descending axons from MesV, mouse embryos were cultured in vitro. Embryos were harvested from timed pregnant CD1 mice at E9.0 and maintained in vitro for 4 days (E9/DIV4: 4 liters—12 embryo cultures in total). All embryos continued to develop as judged by heartbeat and the development of the neural tube, spinal and cranial nerves, etc. (Fig. 7). The overall appearance of the axon tracts in the immunoperoxidase-stained E9/DIV4 embryos is not as precise as in their age-matched counterparts in vivo, but most landmarks can be identified and it is clear that significant further development occurred in vitro, perhaps to the E11/E12 stage. For example, at E9, the vestibular ganglia have not yet developed (see Fig. 3c), but in E9/DIV4 embryos the trochlear and oculomotor nerves—not yet present at E9 (see Fig. 3a)—have now formed (compare in vivo—Figs. 2b and

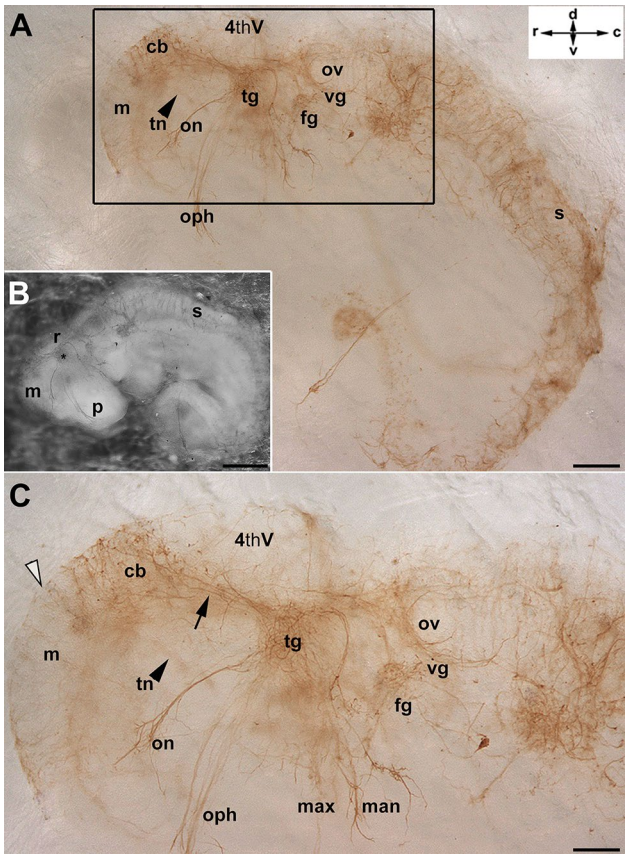

Fig. 7 Whole mount culture of a normal E9 mouse embryo maintained 4 days in vitro (E9/DIV4) and immunoperoxidase stained for NAA. **a** Anti-NAA immunoperoxidase staining of the E9/DIV4 embryo (shown in bright field in **b**) shows that the spinal and cranial nerves continue to develop in vitro. **c** A higher magnification view of the same E9/DIV4 embryo shows well-developed cranial nerves and the cerebellar primordium. The location of the trochlear nerve (out of the plane of focus in this image) marks the mesencephalic/metencephalic boundary (indicated by an arrowhead). The arrow indicates the projection from the trigeminal ganglion (tg) to the cerebellar primordium (cb). No NAA immunoreactivity is present rostral to the mesencephalic/metencephalic boundary (arrowhead: in particular, the MesV is not immunostained—compared to Fig. 5). Other abbreviations: *4thV* 4th ventricle, *fg* facial ganglion, *man* mandibular nerve, *max* maxillary nerve, *m* mesencephalon, *on* oculomotor nerve, *oph* ophthalmic nerve, *ov* otic vesicle, *p* prosencephalon, *s* spinal cord, *tn* trochlear nerve, *vg* vagus ganglion. Scale bars: 500 µm in **a**, **b**; 200 µm in **c**

4a—with in vitro—Fig. 7a, c). Likewise, the ophthalmic, maxillary and mandibular nerve branches of the trigeminal ganglion are not present at E9 (see Figs. 3a and 6a, b), but can all be distinguished in E9/DIV4 embryos [Fig. 7a, c: compared to E11 in vivo (Fig. 4a)]. In particular, the axon tract from the trigeminal ganglion to the cerebellar primordium can be clearly seen (e.g., Fig. 7c, arrow). However, the mesencephalon does not develop normally and the descending axons from MesV to the cerebellar primordium are completely absent (compare the embryos in vivo in Fig. 6a, b with the E9/DIV4 embryo in Fig. 7a, c). Despite the absence of NAA+ axons from MesV, the pathway from the trigeminal ganglion to the cerebellar primordium is well developed (compare Fig. 6a, b to Fig. 7a, c).

The early axons from the trigeminal ganglion terminate on neurons of the developing cerebellar nuclei

Conventionally, it is surmised that the PCs are the targets of the earliest afferents to the cerebellum (Sotelo and Wassef 1991; Kalinovsky et al. 2011). However, the present data show that axons from the trigeminal ganglion have entered the cerebellar primordium by E9, at least a day before the PCs are born at E10–E13 (Miale and Sidman 1961). This points to a novel early stage in cerebellar circuit development and presumably an alternative afferent target field. Given that the PC plate (c2) is not yet formed at E9, when the first afferents are seen, the obvious target within the primordium is the nuclear transitory zone (c3). To test this hypothesis, the PC plate (c2) was identified by Foxp2 immunoreactivity (illustrated at E13 in Fig. 8a), and the nuclear transitory zone (c3) by expression of Tbr1 (Fig. 8b), NAA (Fig. 8c) and Lmx1a (Fig. 9, E12). At E9, double immunofluorescence staining with anti-Lmx1a and anti-NAA shows that NAA+ afferents to the cerebellar primordium are concentrated in the newly formed Lmx1a+ c3 domain (Fig. 9a–c). The same distribution is seen at E11 but NAA+ axons have also now entered the newly formed c2 (Figs. 9d–f, 10). To confirm that the target of the early afferents to the cerebellar primordium is c3, similar double immunostaining was performed for NAA and Tbr1. Tbr1 is not expressed in the cerebellar primordium at E9 but by E11 NAA+ fibers are prominent in the Tbr1+ c3. By E12, NAA+ profiles are plentiful in both c2 and c3 (Fig. 9g–i).

The two NAA+ axons fascicles (Fig. 9j) are not simply axons of passage transiting through c3 but rather appear to make intimate contact with Lmx1a+ neurons in the form of finger-like processes reminiscent of axon growth cones (e.g., Fig. 9k, l). Whether these include synaptic contacts is unclear: immunostaining at E12 for the synapse-associated antigens synaptophysin, syntaxin, and PSD-95 revealed no synaptic profiles (data not shown). To confirm and explore this further, we exploited two transcription factors expressed by the newborn PCs in c2—Ptf1a and Foxp2 (Hoshino et al. 2005; Fujita and Sugihara 2012; Hou et al. 2014). As described above, by E11, double immunofluorescence staining of the cerebellar primordium for NAA and either Ptf1a (Fig. 10a–c) or Foxp2 (Fig. 10d–f) shows that NAA+ axons accumulate in c3 and the space between c3 and c2, and then extend into c2. The terminals on the PCs in c2, shown at higher magnification in Fig. 10g and inset, are simple and do not show the extensive envelopment of the cerebellar nuclear

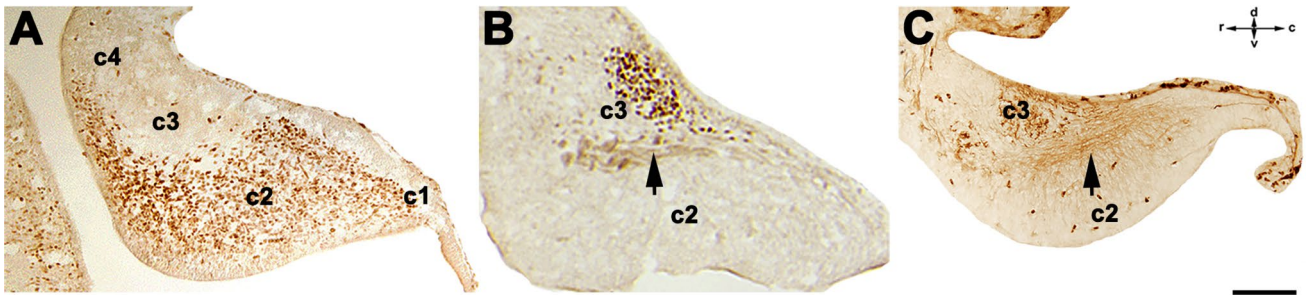

Fig. 8 The regionalization of the embryonic cerebellar primordium. **a** Anti-Foxp2 immunoperoxidase staining of a 20 µm medial sagittal section through the cerebellar primordium at E13 showing strong immunoreactivity in the cells of c2 (the Purkinje cell plate). **b** Anti-Tbr1 immunoperoxidase staining of a 20 µm medial sagittal section through the cerebellar primordium at E13 shows strong immunoreactivity in c3 (the nuclear transitory zone). Weak immunoreactivity is also seen in axons located at the cerebellar core (arrow). **c** Anti-NAA immunoperoxidase staining of a 20 µm sagittal section through the medial cerebellar primordium at E11 shows a strongly immunoreactivity projection to c3 (the nuclear transitory zone) and the cerebellar core (arrow). Scale bar: 500 µm (**a**, **b**)

neurons characteristic of c3. By E12, the number of NAA+ axons in c2 has increased (Fig. 9g–i, arrowheads).

Discussion

The canonical model of early afferent development in mouse is that mossy fiber axons enter the embryonic cerebellar primordium between embryo age E13–E18 and climbing fibers enter the primordium between E14–E15 where they terminate on the PC somata (Sotelo and Wassef 1991; Kalinovsky et al. 2011; Sillitoe 2016) (reviewed in Rahimi-Balaei et al. 2015). The earliest reported mossy fiber afferents to the cerebellum are the central processes of the vestibular ganglion neurons (Morris et al. 1988; Ashwell and Zhang 1992, 1998): the neurons of the vestibular ganglia are born on E10–E14 (Ruben 1967) and afferents from the vestibular nuclei to the cerebellum are first observed (at E15 in rat: Morris et al. 1988).

In the present study, we describe a novel, earlier step in the formation of cerebellar afferent topography—a direct axonal pathway from the trigeminal ganglion to the cerebellar primordium at E9 (Fig. 3). This is a day before PCs are first born and so at E9, the afferents' targets cannot be PCs. Rather, the primary targets of the trigeminal ganglion appear to be the nascent c3 neurons of the cerebellar nuclei (Fig. 9: CN neurons in c3 are born from E9–E12: Miale and Sidman 1961). It is not certain that the axons in c2 and to c3 arise from a common neuronal population. For example, it is possible that the early axons that innervate c3 derive from the trigeminal ganglion, but the later c2 innervation arises from a different source, such as the vestibular ganglia. That is, it cannot be determined if c3 is a synaptic target of the trigeminal ganglion afferents or if the trigeminal afferents, arriving so early, enter c3 *faute de mieux* and are merely axons of passage. The NAA+ innervation of c3 involves elaborate interactions with the CN neurons (e.g., Fig. 9), so the afferents do not appear to be simply axons of passage, although no synapses have been detected at this stage. Subsequently, NAA+ axons also invade c2 (E10–E11). The absence of NAA+ axons in the cerebellar primordium of the *Neurog1*$^{-/-}$ mouse (Fig. 6) plus the presence of multiple branching axons in the E11 tract (Fig. 5) are consistent with an interpretation that the c2 innervation is part of the same axon tract that innervates c3, but a second source—for example, the vestibular ganglion—cannot be excluded. Indeed, by E11, two distinct NAA+ fascicles are present in the primordium (e.g., Fig. 4). It is not clear if both derive from the trigeminal ganglion or if the later-forming deep fascicle is vestibular as both are missing in the *Neurog1*$^{-/-}$ brain, the early afferents cannot be vestibular—the vestibular ganglia are not yet formed.

Because the NAA+ axon tract at E9 extends from the trigeminal ganglion across the alar plate of rhombomere 1 (the cerebellar primordium), and beyond the isthmus to the mesencephalon, it was important to distinguish descending axons from MesV from ascending axons from the trigeminal ganglion as the source of the earliest cerebellar afferents. To this end, a combination of DiI tracing, *Neurog1* null mice and embryo cultures was deployed. First, DiI tracing supported the proposition that there is a direct embryonic axonal connection between the trigeminal ganglion and the cerebellar primordium. Second, we exploited the finding that elimination of *Neurog1* blocks the development of the trigeminal ganglion (e.g., Fig. 6: Ma et al. 1998). The cerebellar primordium in the *Neurog1*$^{-/-}$ mutant lacks NAA+ axons at E9, while the axons from MesV appear normal, suggesting the hypothesis that mesencephalic ganglionic axons are directed toward the trigeminal ganglion using early cerebellar afferents as a substrate. The putative pioneers are presumably trigeminal since the vestibular ganglia are not yet formed (Figs. 3,

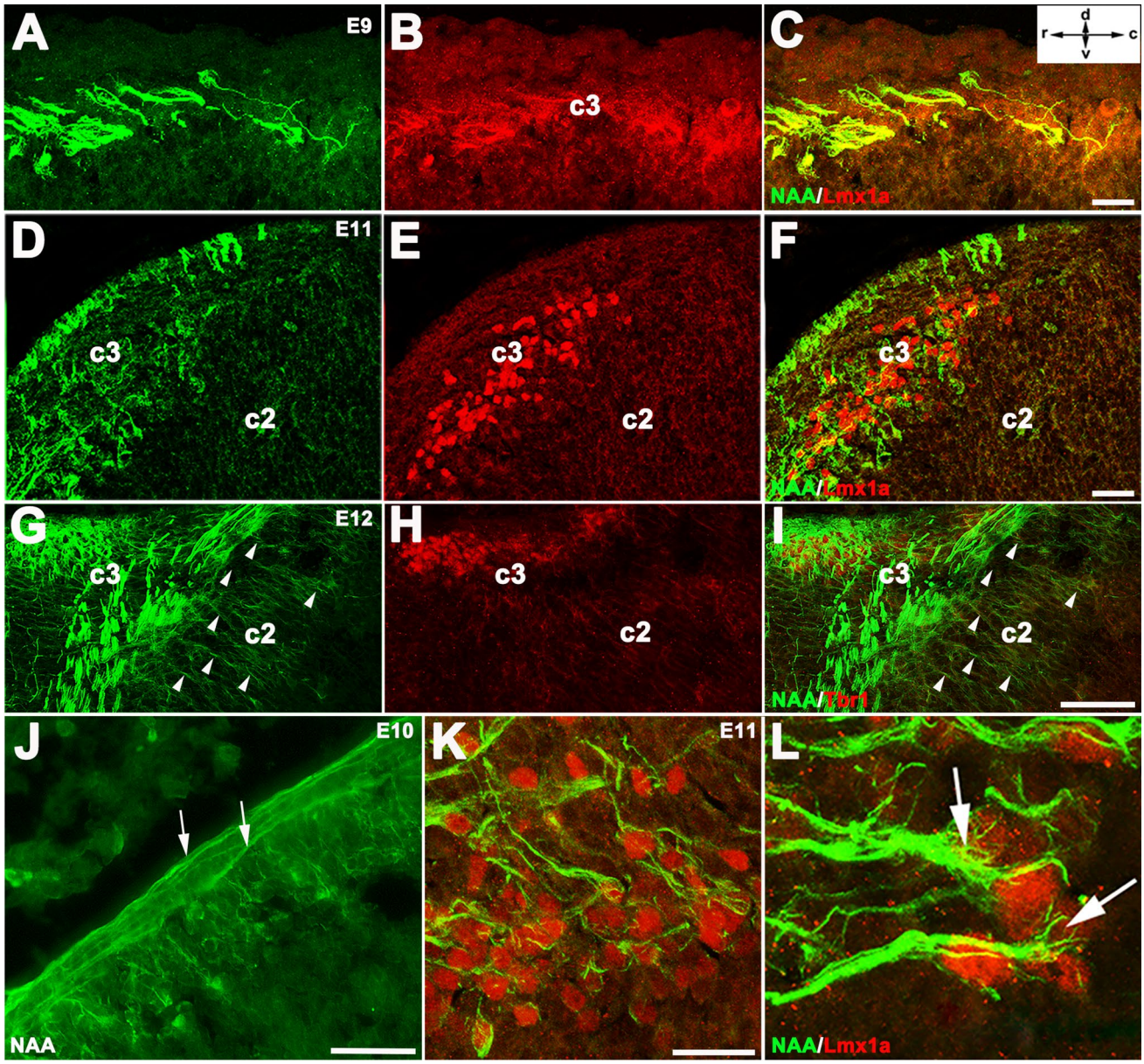

Fig. 9 Double immunofluorescence-stained 20 µm sagittal sections through the cerebellar primordium to show the development of the early afferent terminal fields. **a**–**c** E9 double immunofluorescence staining for NAA (**a**—green) and Lmx1a (**b**—red; **c**—merged) shows that the NAA+ early afferents project to the Lmx1a+c3 (=nuclear transitory zone). **d**–**f** A lateral intermediate sagittal section through the cerebellar primordium at E11 double immunofluorescence stained for NAA (**d**—green) and Lmx1a (**e**—red; **f**—merged). NAA+ afferent axons project to the Lmx1a+ cells in c3. **g**–**i** A medial intermediate sagittal section through the cerebellar primordium at E12 double immunofluorescence stained for NAA (**g**—green) and Tbr1 (**h**—red; **i**—merged) shows the prominent NAA+ afferent to c3 (Tbr1+). Numerous axonal profiles are seen in c2 (arrowhead in **g** and **i**). **j** High magnification image of a lateral sagittal section through the cerebellar primordium at E10. Immunofluorescent staining for NAA shows two fascicles of anti-NAA+ axons (arrows). **k** 20 µm lateral sagittal sections through the E11 cerebellar primordium double immunofluorescence stained for NAA (green) and Lmx1a (red) shows the early afferent axons ramifying throughout c3 (the nuclear transitory zone). **l** Higher magnification image of c3 (rotated compared to the other panels). Double immunofluorescence stained for NAA (green) and Lmx1a (red) shows highly branching axon terminals resembling growth cones (arrows) envelop the somata of the Lmx1a+ neurons. Scale bars: 20 µm in **c** applies to **a**–**c**; 50 µm in **f** applies to **d**–**f**; 100 µm in **i** applies to **g**–**i**; 50 µm in **j**; 25 µm in **k**

6). Third, in cultured E9/DIV4 embryos, NAA+ axons from MesV never develop but the NAA+ tract between the cerebellum and the trigeminal ganglion is nonetheless well developed. This is consistent with the observations of (Stainier and Gilbert 1990), who described ascending afferents from the trigeminal ganglion as early as E9. In

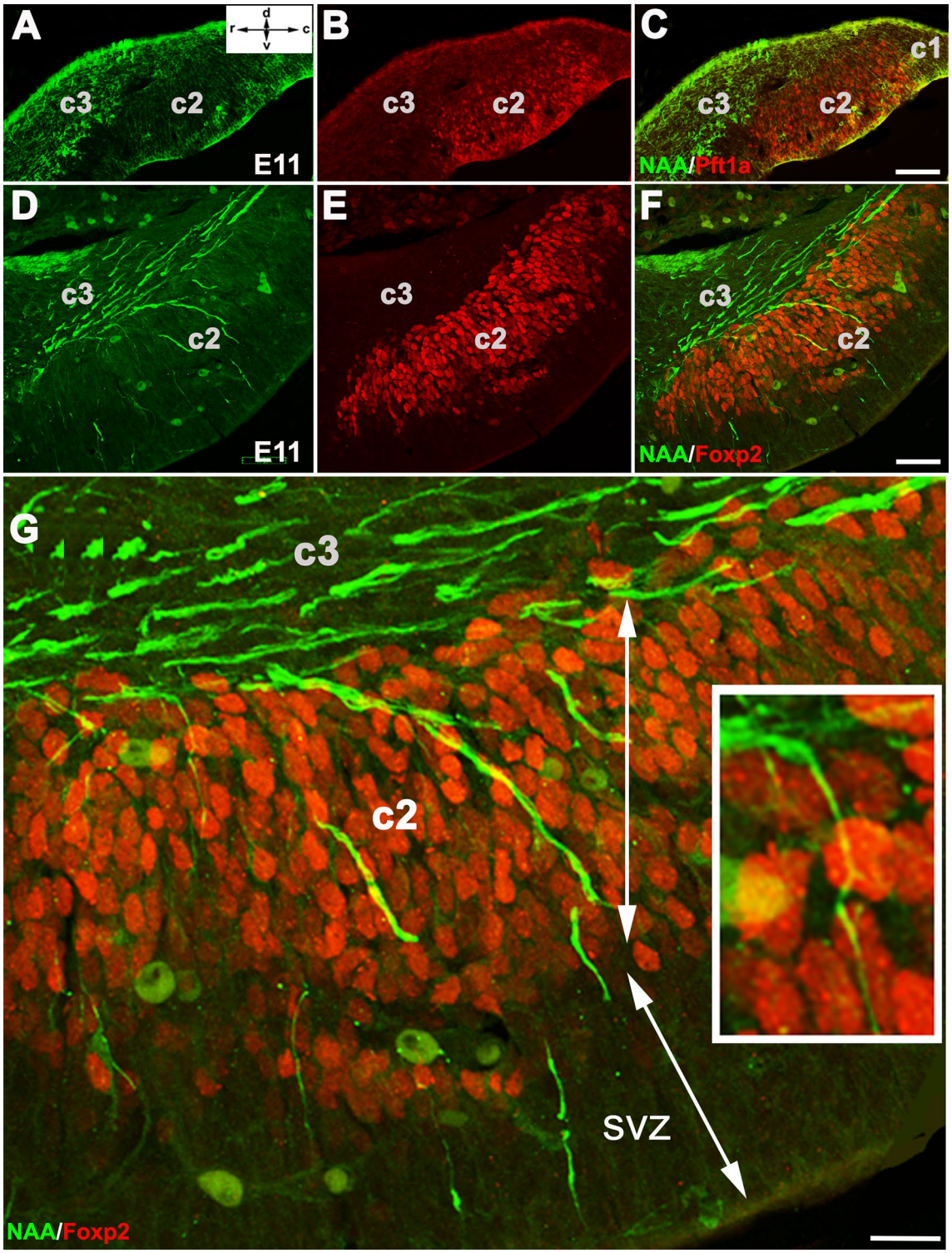

Fig. 10 NAA+ axons to the cerebellar primordium are seen in the Purkinje cell plate (c2) at E11. **a**–**c** A sagittal section through the cerebellar primordium at E11 double immunofluorescence stained for NAA (**a**—green) and Ptf1a (**b**—red; **c**—merged). Most NAA+ axons are still restricted to c3 (these sections are serial to the anti-NAA- and anti-Lmx1a-immunostained sections in Fig. 8d–f). **d**–**f** A sagittal section through the cerebellar primordium at E11 double immunofluorescence stained for NAA (**d**—green) and Foxp2 (**e**—red; **f**—merged) shows axons from c3 extending through the space between c2 and c3 and descending into the Foxp2-immunoreactive c2. **g** A higher power view of the section in **f** to highlight the axons extending from the nuclear transitory zone (c3) into the Purkinje cell plate (c2). In the inset, a single axon is seen—it is slender and unbranched (in contrast to the terminals in c3—see Fig. 8). In a few cases, the axons extend through c2 into the subventricular zone (SVZ). Scattered, large NAA+ somata are also seen in c2: their identity is unknown. Scale bars: 100 µm in **c** applies to **a**–**c**; 50 µm in **f** applies to **d**–**f**; 20 µm in **g**

summary, the data support the hypothesis that cerebellar afferents entering the cerebellar primordium at E9 originate in the trigeminal ganglion, run rostrally close to the pial surface, and then enter the cerebellar primordium. It is not clear whether these earliest afferents serve as pioneers in the sense of guiding subsequent cerebellar afferents, a role proposed previously for both vestibulocerebellar (Morris et al. 1988) and trigeminocerebellar afferents (Rochlin and Farbman 1998; Stainier and Gilbert 1990; Lumsden and Davies 1983). It is clear that trigeminal afferents do play such a role elsewhere in the developing brain (e.g., Lumsden and Davies 1983; Moody and Heaton 1983). In principle, analysis of later afferent topography in the *Neurog1*$^{-/-}$ would begin to address this, but such experiments are complicated as the mutant is embryonic lethal.

We have avoided calling the direct trigeminal ganglion–cerebellar primordium projection a "mossy fiber" pathway, because we are uncertain as to whether the tract is preserved in the adult animal or is only present transiently during embryogenesis, in which case a mossy fiber phenotype is moot. A direct mossy fiber projection from the trigeminal ganglion, via the restiform body to the hemispheres and lateral cerebellar nuclei, has been reported in rat (Jacquin et al. 1982; Marfurt and Rajchert 1991) and it may be that this is the adult version of the embryonic pathway described here, in which case the trigeminal ganglion projection is indeed a mossy fiber pathway. Alternatively, it may be a transient pathway, for example, serving a pioneer role for later-arriving axons—axons of the mouse trigeminal ganglion do seem to perform such a pioneer role in the periphery (Stainier and Gilbert 1990), and substantial pruning of the early vestibulocerebellar afferents has been described in rat (Ashwell and Zhang 1998).

Finally, an adult cerebellar module comprises a PC stripe projecting to a CN subregion, and with both innovated by a common climbing and mossy fiber afferent subset (e.g., reviewed in Voogd and Ruigrok 2004; Apps et al. 2018). In this fashion, mossy and climbing fibers to the cerebellum are typically thought of as having a primary projection to the PCs and collateral branches to the CN, however, if other embryonic afferent pathways also first target CN neurons rather than PCs, then perhaps we should refer to the CN projections as the "primary" afferent projections, with the cerebellar cortical projections to the PCs as the secondary, "collateral" branches (e.g., Hawkes and Gravel 1991).

Acknowledgements These studies were supported by grants from the Natural Sciences and Engineering Research Council (HM: NSERC Discovery Grant # RGPIN-2018-06040) and the Canadian Institutes of Health Research (RH). We are most grateful to Dr. Carol Schuurmans (U. Toronto) for *Neurog1* null mouse stocks and to Drs. M. German (UCSF) and H. Edlund (Umeå, Sweden) for antibodies, and Dr. S. McFarlane for her advice on an earlier draft.

Compliance with ethical standards

Conflict of interest The authors declare that they have no conflict of interest.

Subjects All studies were conducted on CD1, and neurogenin1 (*Neurog1*) null mutant mice, and E9–E13 embryos from timed pregnant CD1.

Ethical approval All procedures for the handling and experimental use of animals were conducted in accordance with institutional regulations and the Guide to the Care and Use of Experimental Animals from the Canadian Council for Animal Care and have been approved by local authorities "the Bannatyne Campus Animal Care Committee" (approved protocol # 15066). This article does not contain any studies with human participants performed by any of the authors.

Informed consent All studies were conducted on mice.

References

Akazawa C, Ishibashi M, Shimizu C, Nakanishi S, Kageyama R (1995) A mammalian helix–loop–helix factor structurally related to the product of Drosophila proneural gene atonal is a positive transcriptional regulator expressed in the developing nervous system. J Biol Chem 270:8730–8738

Altman J, Bayer SA (1985) Embryonic development of the rat cerebellum. I. Delineation of the cerebellar primordium and early cell movements. J Comp Neurol 231:1–26

Apps R, Hawkes R (2009) Cerebellar cortical organization: a one-map hypothesis. Nat Rev Neurosci 10:670–681

Apps R, Hawkes R, Aoki S, Bengtsson F, Brown AM, Chen G, Ebner TJ, Isope P, Jorntell H, Lackey EP, Lawrenson C, Lumb B, Schonewille M, Sillitoe RV, Spaeth L, Sugihara I, Valera A, Voogd J, Wylie DR, Ruigrok TJH (2018) Cerebellar modules and their role as operational cerebellar processing units. Cerebellum 17:654–682

Ashwell KW, Zhang LL (1992) Ontogeny of afferents to the fetal rat cerebellum. Acta Anat (Basel) 145:17–23

Ashwell KW, Zhang LI (1998) Prenatal development of the vestibular ganglion and vestibulocerebellar fibres in the rat. Anat Embryol (Berl) 198:149–161

Bailey K, Rahimi Balaei M, Mannan A, Del Bigio MR, Marzban H (2014) Purkinje cell compartmentation in the cerebellum of the lysosomal Acid phosphatase 2 mutant mouse (nax—naked-ataxia mutant mouse). PLoS One 9:e94327

Billig I, Yatim N, Compoint C, Buisseret-Delmas C, Buisseret P (1995) Cerebellar afferences from the mesencephalic trigeminal nucleus in the rat. NeuroReport 6:2293–2296

Bovolenta P, Mallamaci A, Briata P, Corte G, Boncinelli E (1997) Implication of OTX2 in pigment epithelium determination and neural retina differentiation. J Neurosci 17:4243–4252

Cai J, Donaldson A, Yang M, German MS, Enikolopov G, Iacovitti L (2009) The role of Lmx1a in the differentiation of human embryonic stem cells into midbrain dopamine neurons in culture and after transplantation into a Parkinson's disease model. Stem Cells 27:220–229

Chizhikov V, Steshina E, Roberts R, Ilkin Y, Washburn L, Millen KJ (2006) Molecular definition of an allelic series of mutations disrupting the mouse Lmx1a (dreher) gene. Mamm Genome 17:1025–1032

Crepel F (1982) Regression of functional synapses in the immature mammalian cerebellum. Trends Neurosci 5:266–269

Erzurumlu RS, Jhaveri S (1992) Trigeminal ganglion cell processes are spatially ordered prior to the differentiation of the vibrissa pad. J Neurosci 12:3946–3955

Failli V, Bachy I, Retaux S (2002) Expression of the LIM-homeodomain gene Lmx1a (dreher) during development of the mouse nervous system. Mech Dev 118:225–228

Fink AJ, Englund C, Daza RA, Pham D, Lau C, Nivison M, Kowalczyk T, Hevner RF (2006) Development of the deep cerebellar nuclei: transcription factors and cell migration from the rhombic lip. J Neurosci 26:3066–3076

Fode C, Gradwohl G, Morin X, Dierich A, Lemeur M, Goridis C, Guillemot F (1998) The bHLH protein NEUROGENIN 2 is a determination factor for epibranchial placode-derived sensory neurons. Neuron 20:483–494

Fujita H, Sugihara I (2012) FoxP2 expression in the cerebellum and inferior olive: development of the transverse stripe-shaped expression pattern in the mouse cerebellar cortex. J Comp Neurol 520:656–677

Hamburger V (1961) Experimental analysis of the dual origin of the trigeminal ganglion in the chick embryo. J Exp Zool 148:91–123

Hashimoto K, Kano M (2013) Synapse elimination in the developing cerebellum. Cell Mol Life Sci 70:4667–4680

Hawkes R, Gravel C (1991) The modular cerebellum. Prog Neurobiol 36:309–327

Hoshino M, Nakamura S, Mori K, Kawauchi T, Terao M, Nishimura YV, Fukuda A, Fuse T, Matsuo N, Sone M, Watanabe M, Bito H, Terashima T, Wright CV, Kawaguchi Y, Nakao K, Nabeshima Y (2005) Ptf1a, a bHLH transcriptional gene, defines GABAergic neuronal fates in cerebellum. Neuron 47:201–213

Hou C, Ding L, Zhang J, Jin Y, Sun C, Li Z, Sun X, Zhang T, Zhang A, Li H, Gao J (2014) Abnormal cerebellar development and Purkinje cell defects in Lgl1-Pax2 conditional knockout mice. Dev Biol 395:167–181

Jacquin MF, Semba K, Rhoades RW, Egger MD (1982) Trigeminal primary afferents project bilaterally to dorsal horn and ipsilaterally to cerebellum, reticular formation, and cuneate, solitary, supratrigeminal and vagal nuclei. Brain Res 246:285–291

Kalinovsky A, Boukhtouche F, Blazeski R, Bornmann C, Suzuki N, Mason CA, Scheiffele P (2011) Development of axon-target specificity of ponto-cerebellar afferents. PLoS Biol 9:e1001013

Karpinski BA, Bryan CA, Paronett EM, Baker JL, Fernandez A, Horvath A, Maynard TM, Moody SA, Lamantia AS (2016) A cellular and molecular mosaic establishes growth and differentiation states for cranial sensory neurons. Dev Biol 415:228–241

Kim JY, Marzban H, Chung SH, Watanabe M, Eisenman LM, Hawkes R (2009) Purkinje cell compartmentation of the cerebellum of microchiropteran bats. J Comp Neurol 517:193–209

Lai CS, Gerrelli D, Monaco AP, Fisher SE, Copp AJ (2003) FOXP2 expression during brain development coincides with adult sites of pathology in a severe speech and language disorder. Brain 126:2455–2462

Lassiter RN, Stark MR, Zhao T, Zhou CJ (2014) Signaling mechanisms controlling cranial placode neurogenesis and delamination. Dev Biol 389:39–49

Leto K, Arancillo M, Becker EB, Buffo A, Chiang C, Ding B, Dobyns WB, Dusart I, Haldipur P, Hatten ME, Hoshino M, Joyner AL, Kano M, Kilpatrick DL, Koibuchi N, Marino S, Martinez S, Millen KJ, Millner TO, Miyata T, Parmigiani E, Schilling K, Sekerkova G, Sillitoe RV, Sotelo C, Uesaka N, Wefers A, Wingate RJ, Hawkes R (2016) Consensus paper: cerebellar development. Cerebellum 15:789–828

Li H, Edlund H (2001) Persistent expression of Hlxb9 in the pancreatic epithelium impairs pancreatic development. Dev Biol 240:247–253

Lin B, Wang SW, Masland RH (2004) Retinal ganglion cell type, size, and spacing can be specified independent of homotypic dendritic contacts. Neuron 43:475–485

Lugani F, Arora R, Papeta N, Patel A, Zheng Z, Sterken R, Singer RA, Caridi G, Mendelsohn C, Sussel L, Papaioannou VE, Gharavi AG (2013) A retrotransposon insertion in the 5′ regulatory domain of Ptf1a results in ectopic gene expression and multiple congenital defects in Danforth's short tail mouse. PLoS Genet 9:e1003206

Lumsden AG, Davies AM (1983) Earliest sensory nerve fibres are guided to peripheral targets by attractants other than nerve growth factor. Nature 306:786–788

Ma Q, Chen Z, Del Barco Barrantes I, De la Pompa JL, Anderson DJ (1998) Neurogenin1 is essential for the determination of neuronal precursors for proximal cranial sensory ganglia. Neuron 20:469–482

Ma Q, Fode C, Guillemot F, Anderson DJ (1999) Neurogenin1 and neurogenin2 control two distinct waves of neurogenesis in developing dorsal root ganglia. Genes Dev 13:1717–1728

Ma Q, Anderson DJ, Fritzsch B (2000) Neurogenin 1 null mutant ears develop fewer, morphologically normal hair cells in smaller sensory epithelia devoid of innervation. J Assoc Res Otolaryngol 1:129–143

Machold R, Fishell G (2005) Math1 is expressed in temporally discrete pools of cerebellar rhombic-lip neural progenitors. Neuron 48:17–24

Marfurt CF, Rajchert DM (1991) Trigeminal primary afferent projections to "non-trigeminal" areas of the rat central nervous system. J Comp Neurol 303:489–511

Marzban H, Kim CT, Doorn D, Chung SH, Hawkes R (2008) A novel transverse expression domain in the mouse cerebellum revealed by a neurofilament-associated antigen. Neuroscience 153:1190–1201

Marzban H, Del Bigio MR, Alizadeh J, Ghavami S, Zachariah RM, Rastegar M (2014) Cellular commitment in the developing cerebellum. Front Cell Neurosci 8:450

Miale IL, Sidman RL (1961) An autoradiographic analysis of histogenesis in the mouse cerebellum. Exp Neurol 4:277–296

Moody SA, Heaton MB (1983) Developmental relationships between trigeminal ganglia and trigeminal motoneurons in chick embryos. II. Ganglion axon ingrowth guides motoneuron migration. J Comp Neurol 213:344–349

Moody SA, Quigg MS, Frankfurter A (1989) Development of the peripheral trigeminal system in the chick revealed by an isotype-specific anti-beta-tubulin monoclonal antibody. J Comp Neurol 279:567–580

Morris RJ, Beech JN, Heizmann CW (1988) Two distinct phases and mechanisms of axonal growth shown by primary vestibular fibres in the brain, demonstrated by parvalbumin immunohistochemistry. Neuroscience 27:571–596

Rahimi-Balaei M, Afsharinezhad P, Bailey K, Buchok M, Yeganeh B, Marzban H (2015) Embryonic stages in cerebellar afferent development. Cerebellum Ataxias 2:7

Reeber SL, White JJ, George-Jones NA, Sillitoe RV (2012) Architecture and development of olivocerebellar circuit topography. Front Neural Circuits 6:115

Riccomagno MM, Kolodkin AL (2015) Sculpting neural circuits by axon and dendrite pruning. Annu Rev Cell Dev Biol 31:779–805

Rochlin MW, Farbman AI (1998) Trigeminal ganglion axons are repelled by their presumptive targets. J Neurosci 18:6840–6852

Ruben RJ (1967) Development of the inner ear of the mouse: a radioautographic study of terminal mitoses. Acta Otolaryngol Suppl 220:1–44

Sanders RD (2010) The trigeminal (V) and facial (VII) cranial nerves: head and face sensation and movement. Psychiatry (Edgmont) 7:13–16

Schlosser G (2006) Induction and specification of cranial placodes. Dev Biol 294:303–351

Sillitoe RV (2016) Mossy fibers terminate directly within purkinje cell zones during mouse development. Cerebellum 15:14–17
Sillitoe RV, Hawkes R (2002) Whole-mount immunohistochemistry: a high-throughput screen for patterning defects in the mouse cerebellum. J Histochem Cytochem 50:235–244
Sotelo C, Wassef M (1991) Cerebellar development: afferent organization and Purkinje cell heterogeneity. Philos Trans R Soc Lond B Biol Sci 331:307–313
Stainier DY, Gilbert W (1990) Pioneer neurons in the mouse trigeminal sensory system. Proc Natl Acad Sci USA 87:923–927
Streit A (2004) Early development of the cranial sensory nervous system: from a common field to individual placodes. Dev Biol 276:1–15
Tello JF (1940) Histogenèse du cervelet et ses voies chez la souris blanche. Trab Inst Cajal Investig Biol Madrid 32:1–72
Tischfield MA, Engle EC (2010) Distinct alpha- and beta-tubulin isotypes are required for the positioning, differentiation and survival of neurons: new support for the 'multi-tubulin' hypothesis. Biosci Rep 30:319–330
Voogd J, Ruigrok TJ (2004) The organization of the corticonuclear and olivocerebellar climbing fiber projections to the rat cerebellar vermis: the congruence of projection zones and the zebrin pattern. J Neurocytol 33:5–21
Wang VY, Zoghbi HY (2001) Genetic regulation of cerebellar development. Nat Rev Neurosci 2:484–491
Zordan P, Croci L, Hawkes R, Consalez GG (2008) Comparative analysis of proneural gene expression in the embryonic cerebellum. Dev Dyn 237:1726–1735

Publisher's Note Springer Nature remains neutral with regard to jurisdictional claims in published maps and institutional affiliations.